Bambusuril as Effective Astatide Sequestrator Agent by hydrogen bonding

Clémence Maingueneau, Julie Patissou, Marine Lafosse, Elise Cartier, Jean-François Gestin, Grégory Pieters, Frédéric Taran, Jean-Pierre Dognon, François Guérard and Marie-Pierre Heck

Supporting Information

Table of Contents

1. General Methods and equipment

Commercially available reagents were used without further purification. Bambusuril synthesis were performed under inert atmosphere using anhydrous solvents.

Thin-layer chromatograms (TLC) and flash chromatography separations were respectively performed on precoated silica gel 60 F254 plates (Merck, 0.25 mm, glass or plastic support) and on Merck silica gel 60 (230-400 mesh). TLC on plastic support were revealed by UV Lamp and $KMNO_4$ solution was used for TLC on glass support. RCCs were assessed by TLC analysis of a sample aliquot (DCM/MeOH, 9/1 as eluent) and scanned with a cyclone phosphor imaging scanner (PerkinElmer).

HPLC analysis were carried out on a Waters Alliance e2695 HPLC system equipped with a C4 column (symetry300, 4,6x250 mm, Waters) with UV dectector as a Waters 2489 UV/Vis PDA detector set at λ= 254 nm with the flow rate set at 1.50 mL/min with the following gradient: A=H_2O/0.05% TFA and B=CH_3CN/0.05% TFA ; t=0 min: 90% A 10% B; t=7 min: 30% A 70% B; t=15 min: 100% B.

Microwave synthesis were conducted using a CEM Focused Microwave Discover® SP-X System reactor. The reactions were performed for 2-4 h under magnetic stirring in 10 mL sealed Discovered SP vessels closed with Activent® caps. The Dynamic Control method was used for all microwave reactions where the temperature and the pressure were set (P = 50 W, T = 80 °C, PowerMax on).

^{1}H NMR spectra (400 MHz) and ^{13}C NMR spectra (100 MHz) were recorded on a Bruker Avance 400 MHz spectrometer. Chemical shifts and coupling constants are reported in parts per million (ppm) and in Hertz (Hz) respectively. HRMS and electrospray mass spectra (ESIMS) were obtained from an LCT Premier XE using electro spray ionization coupled with a time flight analyser (ESI-TOF). Electrospray mass spectra were obtained using an ESI-Quadripole autopurify, Waters (pump: 2545, mass: ZQ2000) mass Spectrometer.

2. ITC instrument and procedure

ITC measurements were performed with a VP-ITC microcalorimeter (Microcal, GEHealthcare). Experiments were carried out in methanol at 298.15 ± 0.1 K. Anion binding to BU was investigated via a classical isothermal titration experiment (10 µL additions) and a single injection method (SIM). Injection of solution of sodium iodide was added automatically to the BU solution present in the calorimeter cell while stirring at 307 rpm. Integrated heat effects were analyzed by non-linear regression using a single-site binding model (Microcal Origin 7). The experimental data fitted to a theorical titration curve giving the association constant K_a, the enthalpy of binding ΔH° and the entropy ΔS°. The free energy ΔG° was calculated from the equation: $\Delta G° = \Delta H° - T\Delta S°$, where T is the absolute temperature. The first smaller addition (2 µL), that was used to compensate for diffusion of guest from the injector during equilibration, was discarded prior to data fitting.

3. Synthesis Procedures and characterization data

3a. Tetrabutylammonium bromide @ dodecapropargylbambus[6]uril BU 1

Tetrabutylammonium bromide @ dodecapropargylbambus[6]uril BU 1 was prepared in 45% yield by acidic condensation of diproparglycoluril and *p*-formaldehyde under microwave radiations following our reported procedure.[1]

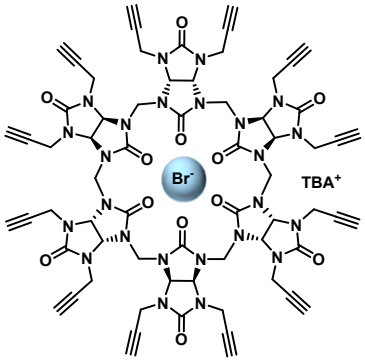

^{1}H NMR (400 MHz, Acetone-D6) δ = 5.82 (12H, s, CH), 5.26 (12H, s, CH_2 bridge), 4.51 (12H, AB syst, J = 2.1, 18.0 Hz, CH_2), 4.44 (12H, AB syst, J = 2.1, 18.0 Hz, CH_2), 3.46 (8H, m, N-**CH_2**-CH_2-CH_2-CH_3), 2.51 (12H, t, J = 2.6 Hz, C≡CH), 1.84 (8H, m, N-CH_2-**CH_2**-CH_2-CH_3), 1.44 (8H, q, J = 7.4 Hz, N-CH_2-CH_2-**CH_2**-CH_3), 0.98 (12H, t, J = 7.4 Hz, N-CH_2-CH_2-CH_2-**CH_3**); ^{13}C NMR (100 MHz, Acetone-D6) δ = 159.7 (C=O), 159.1 (C=O), 81.4 (**C**≡CH), 72.9 (C≡**CH**), 68.0 (CH), 55.0 (N-**CH_2**-CH_2-CH_2-CH_3), 48.5 (CH_2 bridge), 34.4 (CH_2), 24.5 (N-CH_2-**CH_2**-CH_2-CH_3), 20.4 (N-CH_2-CH_2-**CH_2**-CH_3), 13.9 (N-CH_2-CH_2-CH_2-**CH_3**); HRMS (ESI-TOF) m/z [M -TBA + H]$^+$ Calcd for $C_{66}H_{61}BrN_{24}O_{12}$ 1461.4157; found 1461.4155.

3b. Tetrabutylammonium iodide @ dodecapropargylbambus[6]uril BU 2

To a solution of tetrabutylammonium bromide @dodecapropargylbambus[6]uril BU 1 (15 mg, 8.8 mmol, 1 eq.) in CH_3CN (1.5 mL) was added a solution of TBAI in CH_3CN (20 mM/L, 440 µL, 8.8 mmol, 1 eq). Then the reaction was sonicated for 5 min and stirred at RT for 30 min. The solution was concentrated under vacuum to give BU 2 as a yellowish solid (15.4 mg, 98% yield). BU 2 was prepared as well by acidic condensation of dipropargylglycoluril and formaldehyde under microwave radiations following our reported procedure (56% yield).[1]

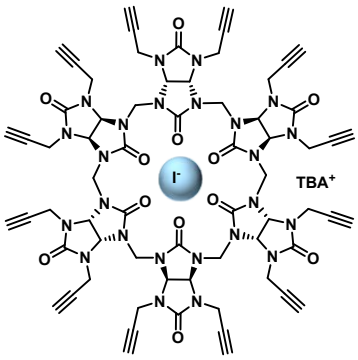

^{1}H NMR (400 MHz, Acetone-D6) δ = 5.93 (12H, s, CH), 5.25 (12H, s, CH_2 bridge), 4.51 (12H, AB syst, J = 2.2, 18.0 Hz, CH_2), 4.46 (12H, AB syst, J = 2.2, 18.0 Hz, CH_2), 3.46 (8H, t, J = 8.6 Hz, N-**CH_2**-CH_2-CH_2-CH_3), 2.52 (12H, t, J = 2.2 Hz, C≡CH), 1.83 (8H, m, N-CH_2-**CH_2**-CH_2-CH_3), 1.44 (8H, q, J = 7.4 Hz, N-CH_2-CH_2-**CH_2**-CH_3), 0.98 (12H, t, J = 7.4 Hz, N-CH_2-CH_2-CH_2-**CH_3**); ^{13}C NMR (100 MHz, Acetone-D6) δ = 159.9 (C=O),

159.4 (C=O), 81.5 (**C**≡CH), 72.9 (C≡**CH**), 68.7 (CH), 59.5 (N-**CH_2**-CH_2-CH_2-CH_3), 48.5 (CH_2 bridge), 34.7 (CH_2), 24.5 (N-CH_2-**CH_2**-CH_2-CH_3), 20.5 (N-CH_2-CH_2-**CH_2**-CH_3), 13.9 (N-CH_2-CH_2-CH_2-**CH_3**); HRMS (ESI-TOF) *m/z* $[M - TBA+H]^+$ Calcd for $C_{66}H_{61}N_{24}O_{12}I$ 1509.4018; found 1509.4012.

3c. ^1H and ^{13}C NMR spectra of bambusurils BU1 and BU2

a) Tetrabutylammonium bromide @Dodecapropargylbambus[6]uril **BU 1** (^1H NMR 400 MHz, Acetone-d6)

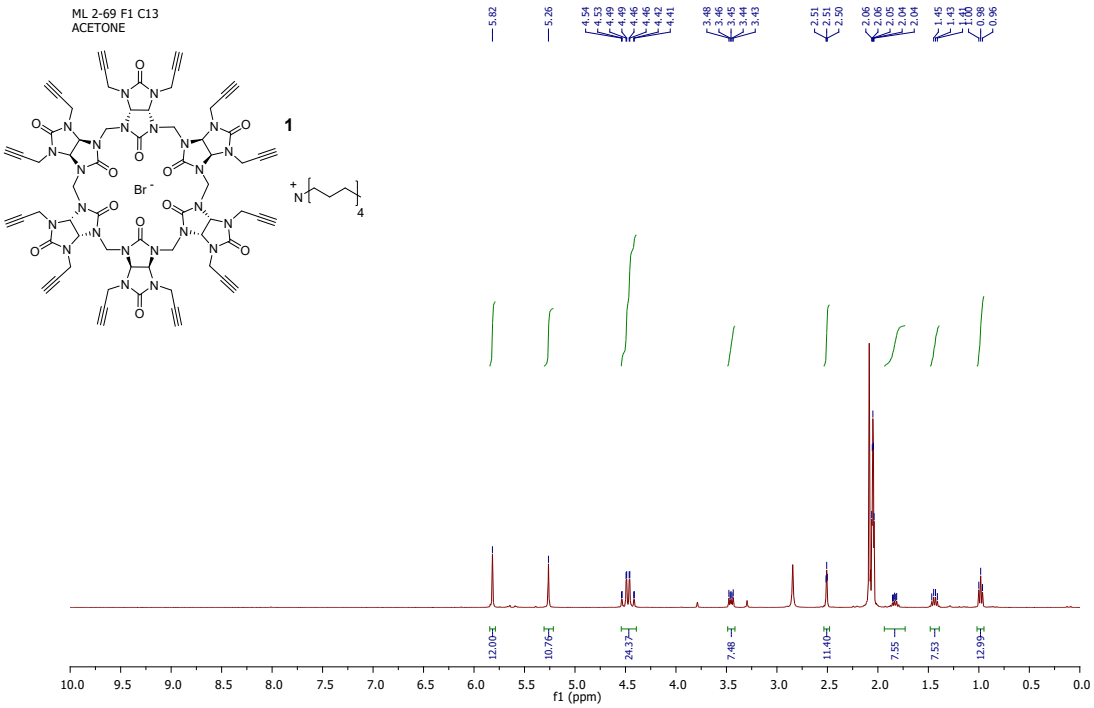

b) Tetrabutylammonium bromide @Dodecapropargylbambus[6]uril **BU 1** (^{13}C NMR 100 MHz, Acetone-d6)

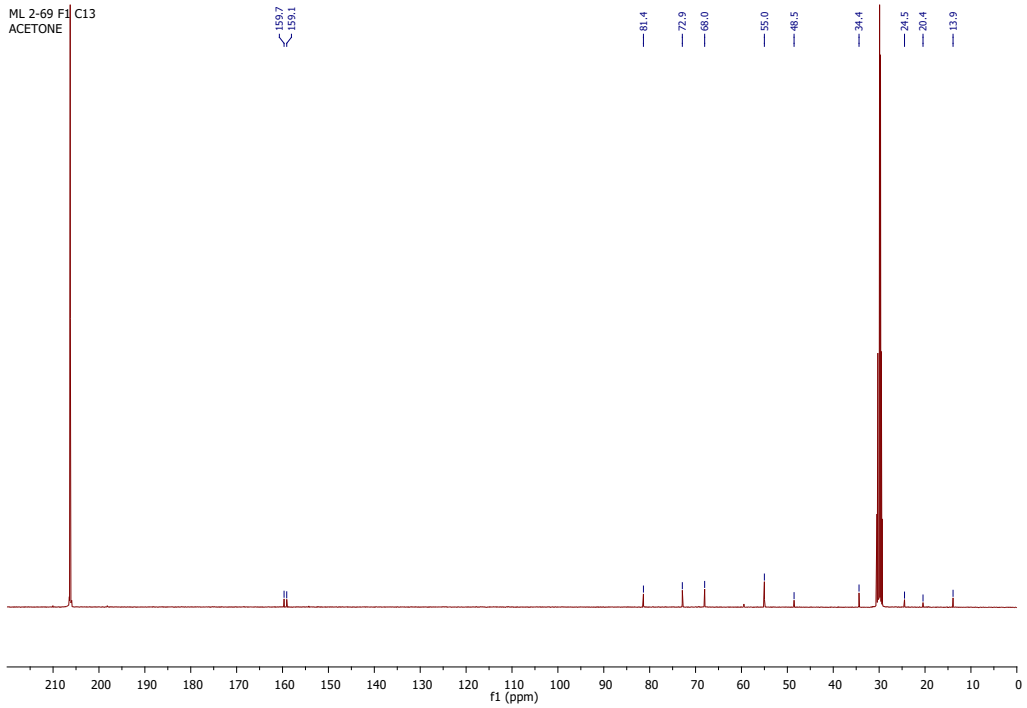

c) Tetrabutylammonium iodide @Dodecapropargylbambus[6]uril **BU 2** (^{1}H NMR 400 MHz, Acetone-d6)

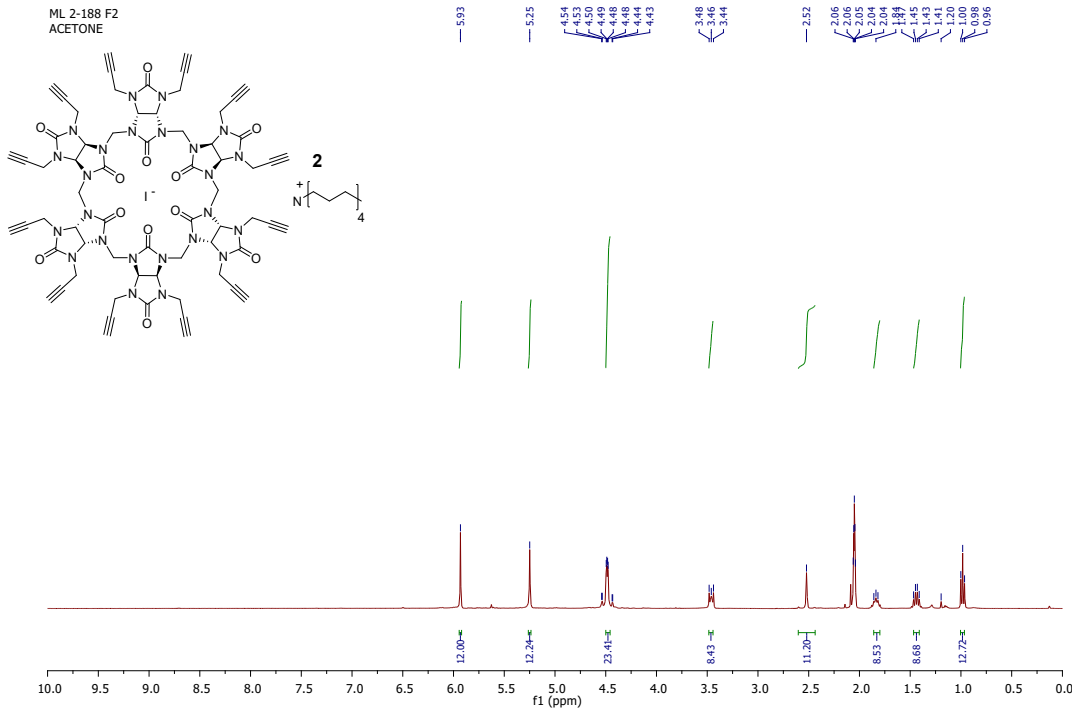

d) Tetrabutylammonium iodide @Dodecapropargylbambus[6]uril **BU 2** (^{13}C NMR 100 MHz, Acetone-d6)

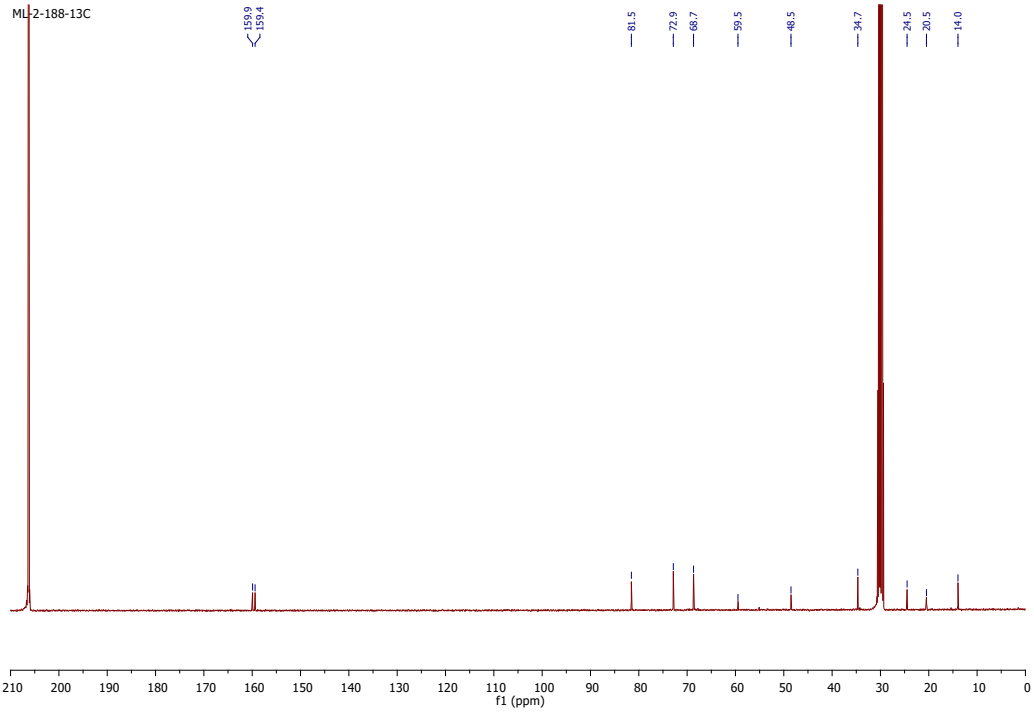

3d Anion-bambusuril titration through NMR ^{1}H spectroscopy

Experiments were recorded at 293.2 K in NMR tubes equipped with Teflon valves from Young Scientific Glassware Ltd, to impede solvent evaporation during NMR experiments. For each addition of small volumes of TBAX solutions, the teflon valve was opened for as short a time as possible.

Previously to each ^{1}H NMR titrations, TBAI salt was solubilized in acetone and then precipitated by addition of diethylether and the obtained TBAI salt was filtred and dried under vacuum to remove water and solvents.

A diluted host solution of propargyl$_{12}$**BU 1** (1 mM) in CD_3CN was prepared and then 400 µL were placed into a NMR tube equipped with Teflon valves. NMR ^{1}H titrations were performed by successive additions of a concentrated (10 mM) solution of TBAI in CD_3CN. After each addition (0.1 to 4 equivalents) of TBAI solution, a ^{1}H NMR was recorded. ^{1}H NMR spectra were calibrated to the residual proton solvent peak in MeCN-D3 (δ = 1.94ppm). Area of signals were obtained by manually integrating signals. Plot stackings were made using MestReNova Version 6.0.

Competition between iodide anions for complexation to Br@propargyl$_{12}$**BU 1** (Figure S1-S2) was performed using integrals of N-CH-N signals characteristic of bromide complex **BU 1** (5.7 ppm) and of iodide complex **BU 2** (5.8 ppm). A 1:1 binding model for iodide anions was used.[2, 3]

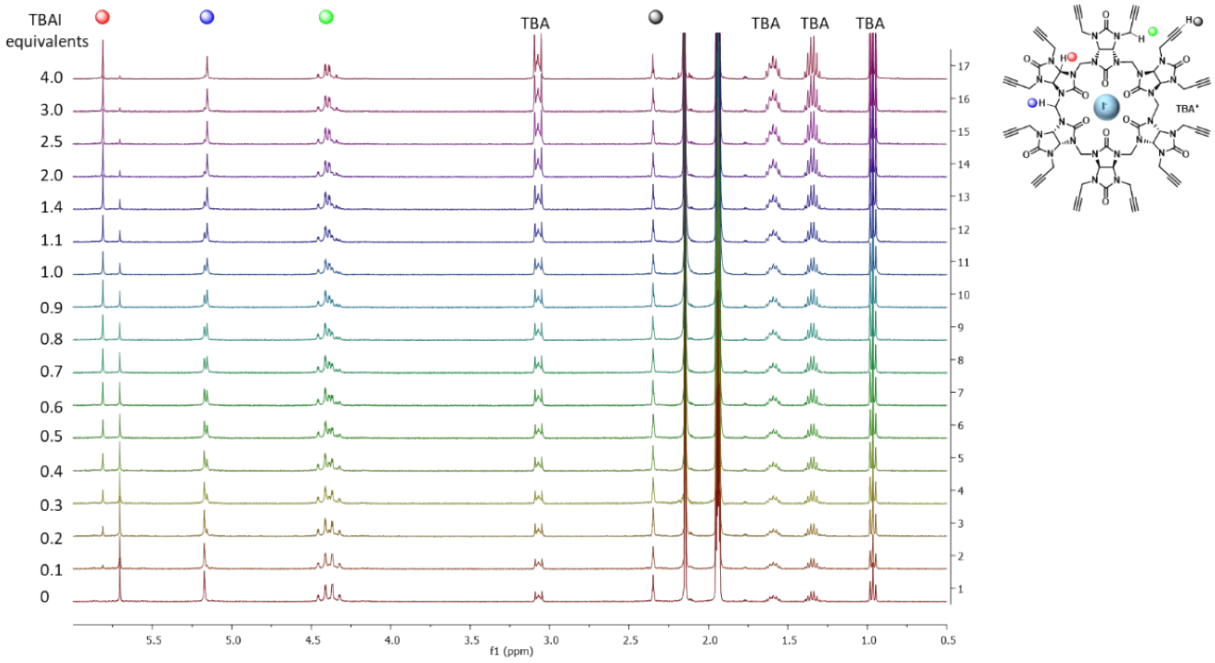

Figure S1: ^{1}H NMR spectra un the course of the titration of Br@Propargyl$_{12}$**BU 1** (1 mM) with TBAI (10 mM) in CD_3CN giving I@Propargyl$_{12}$ **BU 2**

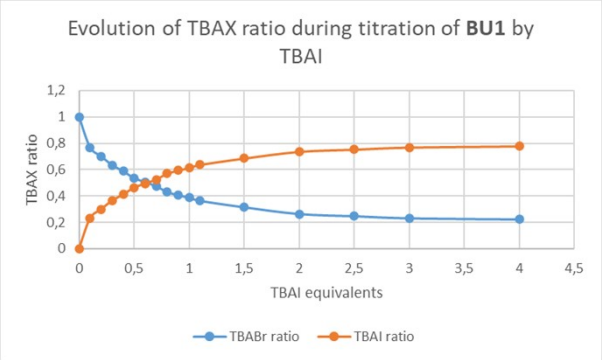

Figure S2: fraction of area of H in **BU 1** in function of TBAI equivalents. The curve is in adequation with a 1:1 model binding and a binding constant K_a was determined (K_a = 4.4 x 10^3 M^{-1} in CD_3CN).

3d. Anion-bambusuril titration through ITC method

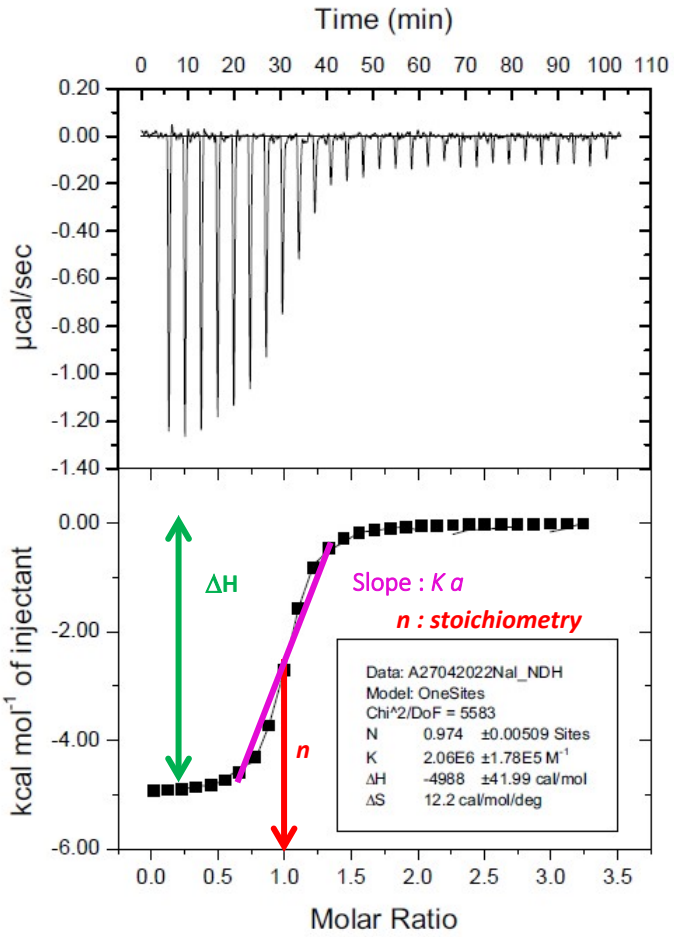

Figure S3: Isothermal titration calorimetry of I^- binding to $(propargyl)_{12}$ **BU 1** in MeOH

Top: Data were obtained from the sequential injections of 10 µL of guest solution (0.6 mM NaI) to **BU 1** (0.05 mM). Bottom: Plot of the total heat released as a function of the total ligand concentration for the titration shown upper. (Indications have been added with colored arrows)

4. Radiolabeling part

4a. Experimental details

Na[^{125}I]I was obtained commercially from Perkin Elmer in 10^{-5} M NaOH solution with a volumic activity of 3.7 MBq/µL). ^{211}At was produced at the Arronax cyclotron facility using the ^{209}Bi (α,2n)^{211}At reaction. Astatine-211 was recovered in chloroform from the irradiated target using a dry-distillation protocol adapted from the reported procedure.[15]

Radio-HPLC analyses were performed using the same HPLC system described above. After the UV detection cell, the system is equipped with a FlowStar LB 513 RadioDetector (Berthold technologies).

The radioTLC yield was assessed by elution of an aliquot deposited on a TLC plate using as eluent DCM/MeOH 9/1. After elution, plates were read using a Cyclone Phosphorimager scanner (Perkin Elmer).

The nonradioactive compound I@**BU 2** was analyzed using the same HPLC system or TLC conditions, its retention time or retention factor was used as reference for identification of its radioiodinated analogue ^{125}I@**BU 3**. Since astatine is a radioelement, it has no stable isotope but it shares similar physical properties with iodine, the identification of ^{211}At@**BU 4** was also realized by the comparison with I@**BU 2** analysis for which retention indexed are expected to be very similar. Radio-HPLC analyses were used for identification of radiolabeled compounds whereas radio-TLC analyses were used for calculation of RCY and RCP in radiolabeling and stability studies, respectively.

4b. Procedure for Astatination of Bambusuril BU 1

Formation of the astatide anion was conducted as follow: the chloroform ^{211}At solution was evaporated to dryness under a gentle stream of nitrogen and dissolved in a volume of a 5 µL of DTT (5 mg/mL in aqueous solution). To the resulting solution was added a solution of bambusuril **BU 1** (45 µL, 0,29 µM) in the appropriated solvent. The solution was stirred at room temperature for 30 min. An aliquot was withdrawn and spotted on TLC plate and another one was diluted in a 1:1 H_2O/CH_3CN solution and analyzed by reverse-phase HPLC.

4c. Preliminary experiments with reducing agents for ^{211}At complexation

On the dry ^{211}At residue (0.5-10 MBq), the appropriated reducing agent was added (Table S1). The obtained solution was vortexed for 30 seconds and 45 µL of bambusuril BU **1** (1,2 mM in CH_3CN) was added, and the mixture was stirred at rt up to 30min. The crude reactions were analyzed on radioTLC.

An additional experiment with ^{211}At and DTT (45 µL MeCN without BU precursor) was performed as control experiment.

Table S 1 : Reducing agents evaluated for ^{211}At complexation with the BU 1

Reducing agent	Solvent	Concentration (mg/mL)	Volume (µL)
Sulfite	H_2O	10	10
Metabisulfite		10	10
DTT		5	5

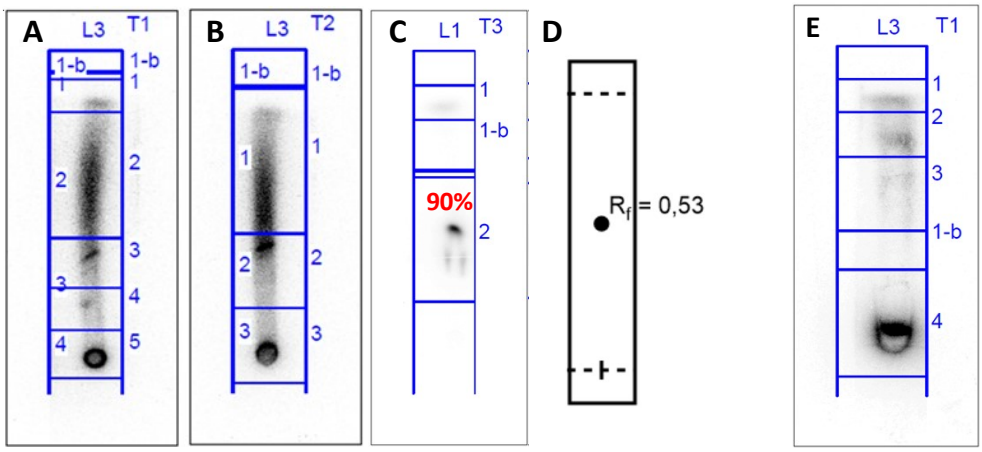

Figure S4: RadioTLC analyses of ^{211}At radiolabeling crude reaction with the **BU 1** in MeCN after 30min depending of the reductive agent: A) sulfite B) metabisulfite C) DTT D) representation of TLC of the **BU 2** eluted in the same condition, E) control experiment with only $^{211}At^-$ + DTT eluted in the same conditions CH_2Cl_2/MeOH 9/1.

4d. Iodination of Bambusuril BU 1

To a solution of diluted Na[^{125}I]I (0.2 MBq-1MBq) from a stock solution of commercially Na[^{125}I]I was added DTT (5 µL, 5 mg/mL in aqueous solution) and the bambusuril **BU 1** (45 µL, 1,2 mM in CH_3CN). The solution was stirred at room temperature for 30 min. An aliquot was withdrawn at the desired time and spotted on TLC plate.

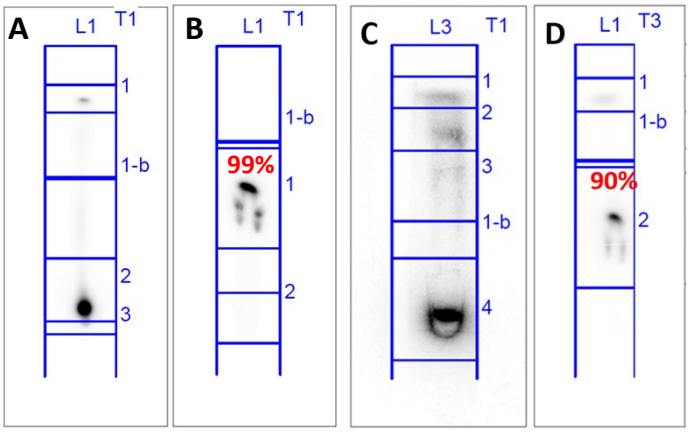

Figure S5: RadioTLC analysis A) control experiment ^{125}I with DTT, B) Crude reaction of ^{125}I complexation with **BU 1** in CH_3CN after 30min, C) control experiment with only$^{211}At^-$ + DTT, D) Crude reaction of ^{211}At complexation with the **BU 1** in MeCN after 30min; elution CH_2Cl_2/MeOH 9/1.

4e. HPLC characterization of ^{125}I@BU 3, ^{211}At@BU 4 and I@ BU 2 complexes

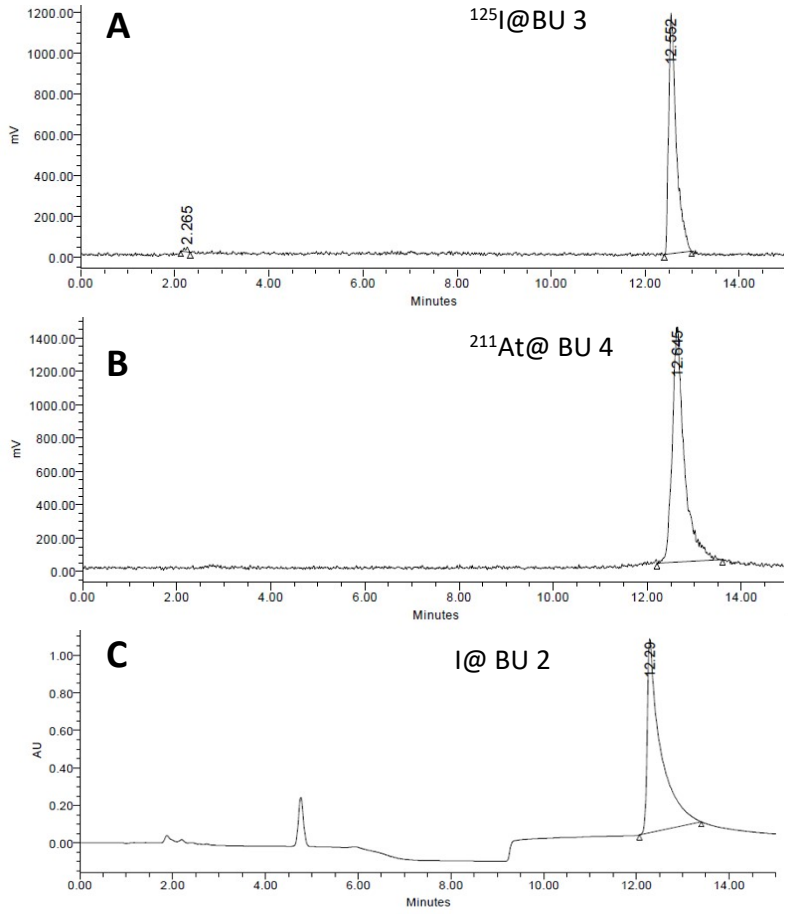

Figure S6: HPLC analysis A) γ trace of the crude reaction of ^{125}I complexation in MeCN after 30 min giving ^{125}I@**BU 3**, B) γ trace of the crude reaction of ^{211}At complexation in CH_3CN after 30 min giving ^{211}At@**BU 4**, C) UV chromatogram of I@**BU 2**

4a. Study of time/solvent/concentration of ^{211}At labeling with BU 1

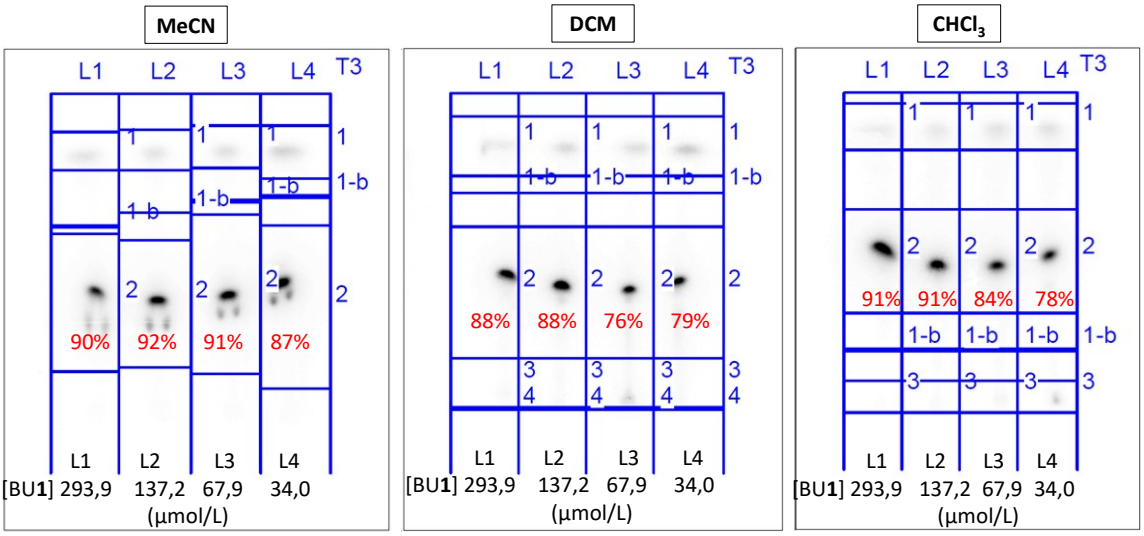

Figure S7: RadioTLC analysis of ^{211}At radiolabeling crude reaction in MeCN, DCM (CH_2Cl_2),$CHCl_3$ solvent after 30 min depending of **BU 1** concentration L1: 293.9 µmol/L; L2: 137.2 µmol/L; L3: 67.9 µmol/L; L4: 34.0 µmol/L; elution CH_2Cl_2/MeOH 9/1.

4b. Study of time/solvent/concentration for ^{125}I labeling with BU 1

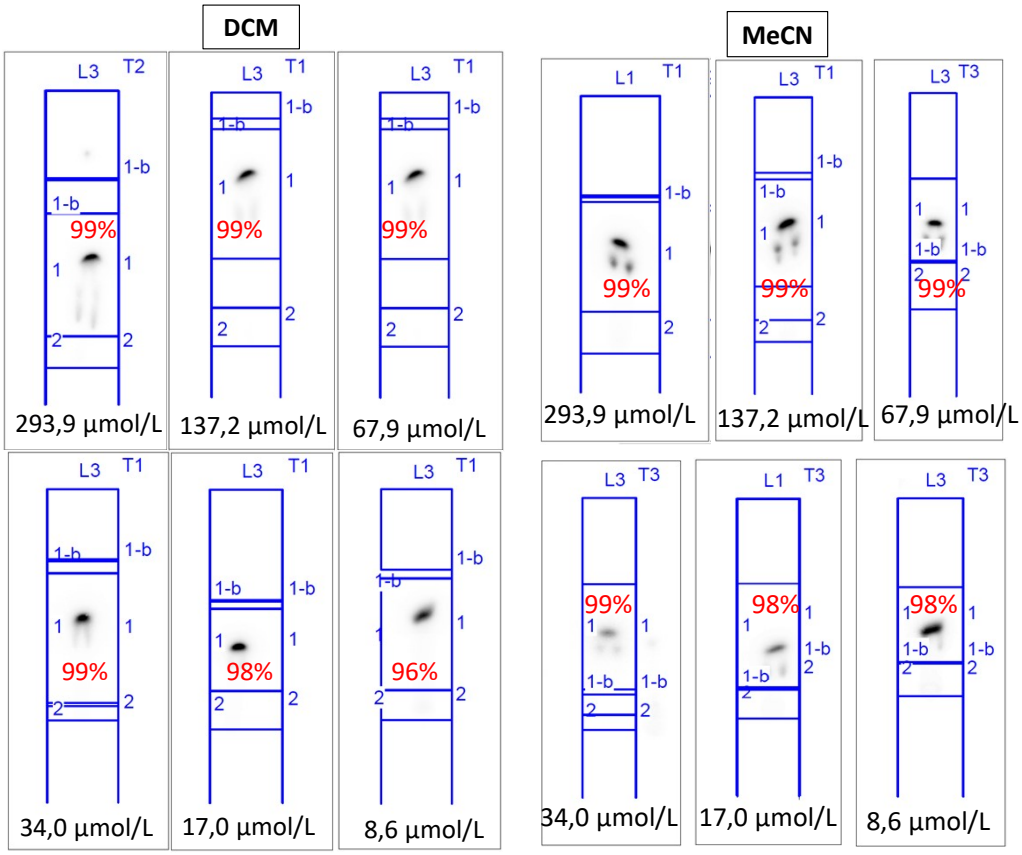

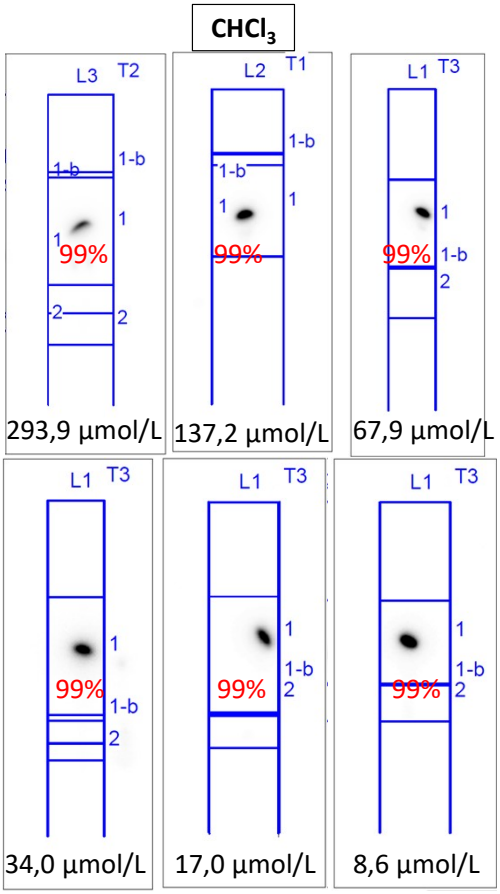

Figure S8: RadioTLC analysis of ^{125}I radiolabeling in MeCN, DCM or $CHCl_3$ after 30 min of reaction with various **BU 1** concentrations; elution CH_2Cl_2/MeOH 9/1.

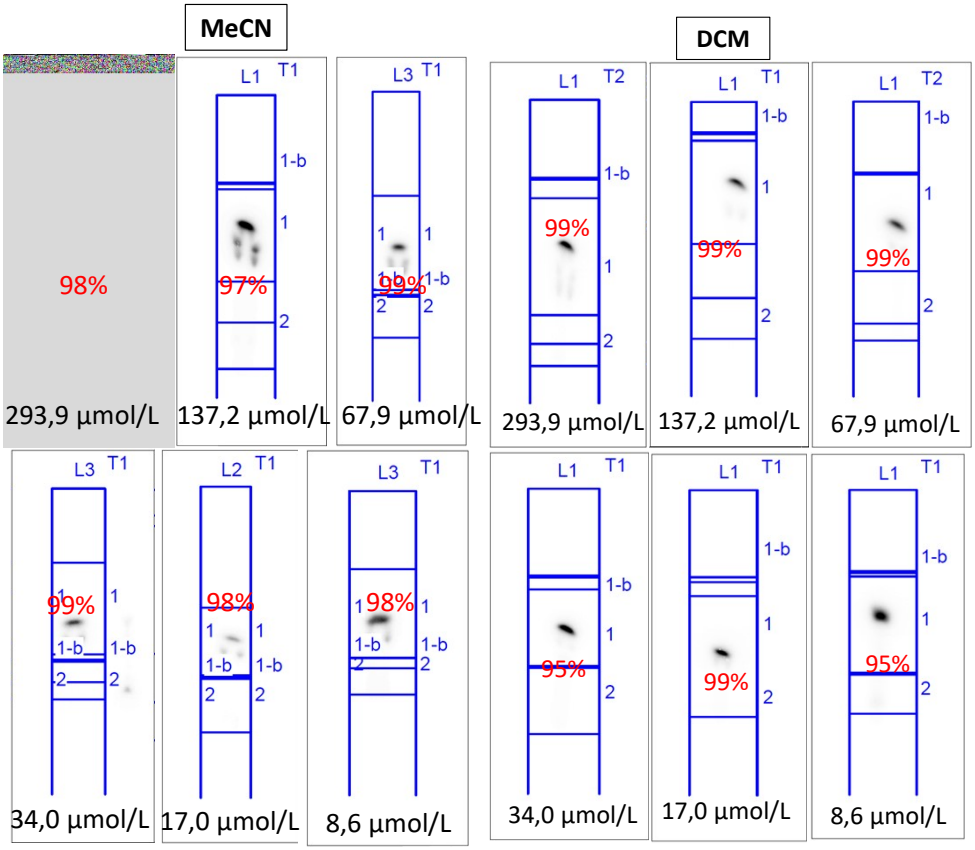

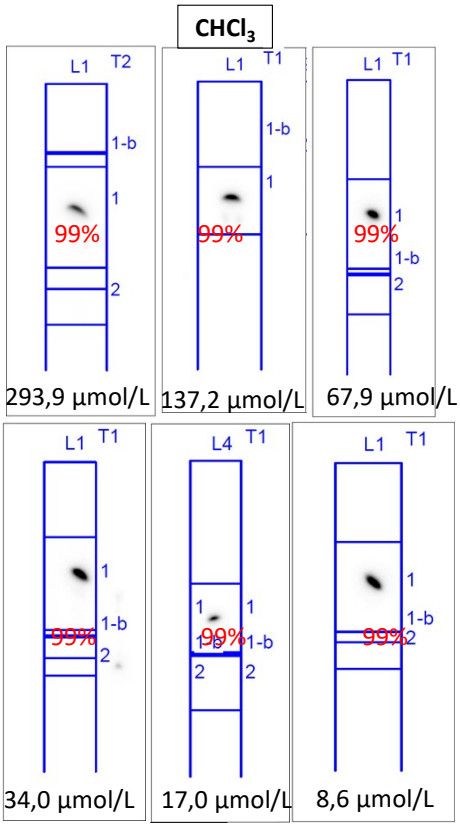

Figure S9: RadioTLC analysis of ^{125}I radiolabeling in $CHCl_3$ after 10 min of reaction with various concentrations of **BU 1**; elution CH_2Cl_2/MeOH 9/1.

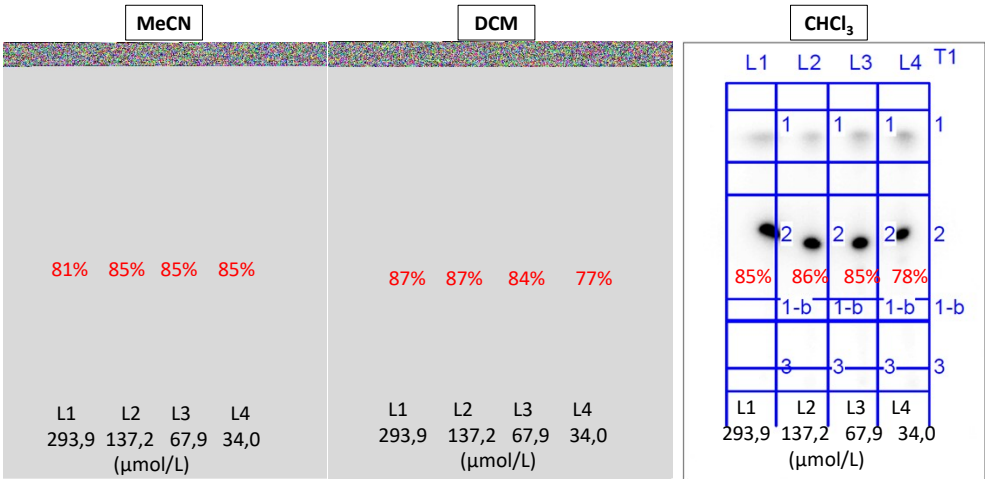

Figure S10: RadioTLC analysis of crude reactions of ^{211}At radiolabeling in MeCN, DCM or $CHCl_3$ after 10 min of reaction with various **BU 1** concentrations L1: 293.9 µmol/L; L2: 137.2 µmol/L; L3: 67.9 µmol/L; L4: 34.0 µmol/L; elution CH_2Cl_2/MeOH 9/1.

5. Purification of Radiolabeled Bambusurils

The crude complex was purified on a cartridge SEP-PAK light silica :the crude mixture was first diluted with DCM (0,5 mL) and then deposited on the cartridge. The cartridge was rinsed with DCM (1,5 mL). ^{125}I@**BU 3** and ^{211}At@**BU 4** were eluted with a solution of DCM/MeOH 9/1 (1 mL). The recovered radiolabeled BUs were then concentrated and diluted with a mixture a 1:1 H_2O/CH_3CN solution and used in stability assays.

6. Stability studies of radiolabeled BUs in PBS

10 µL of the purified radiolabeled BU solution was added to 90 µL of PBS and the resulting mixture was shaken at room temperature. For each analysis point, an aliquot was withdrawn and analyzed in HPLC or TLC.

6a. Stability of ^{125}I@BU 3 in PBS

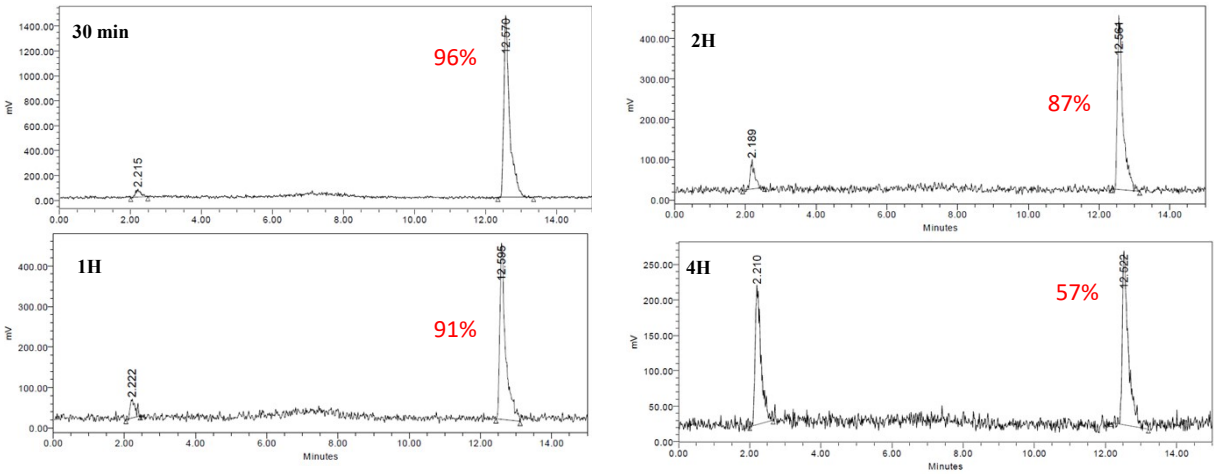

Figure S11: Radio-HPLC analysis of ^{125}I@**BU 3** in PBS at room temperature at 30 min, 1 h, 2 h and 4 hours

6b. Stability of ^{211}At@BU 4 in PBS

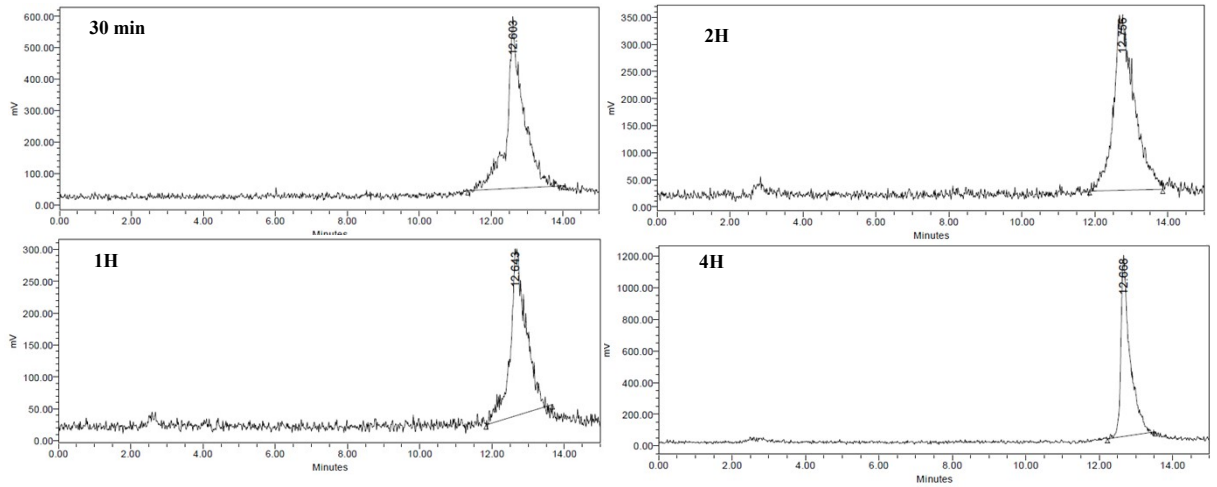

Figure S12a: Radio-HPLC analysis of ^{211}At@**BU 4** in PBS at room temperature from 30 min, 1 h, 2 h, 3h to 4 hours

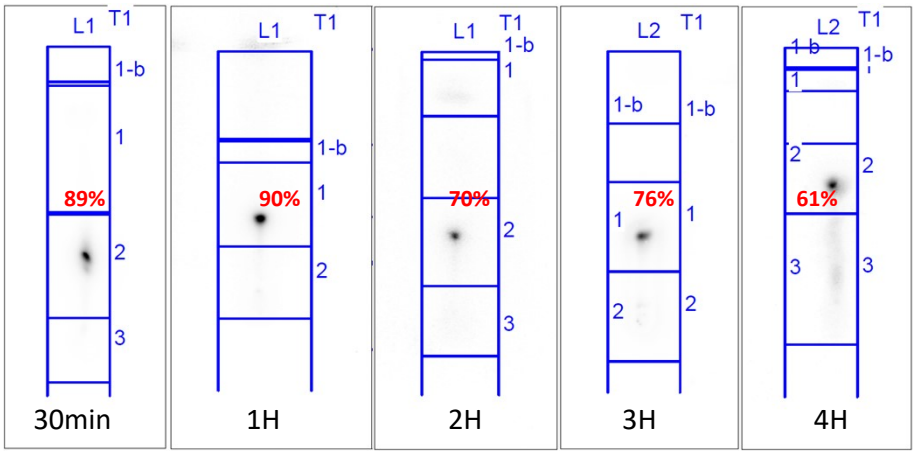

Figure S12b: **Radio-TLC** analysis of ^{211}At@BU 4 in PBS at room temperature for 30 min, 1 h, 2 h to 4 hours (elution with CH_2Cl_2/MeOH : 9/1).

7. Stability studies of radiolabeled BUs in Human Serum

10 µL of purified radiolabeled BU solution was added to 90 µL of human serum (HS). After shaking vigorously for a few seconds, the mixture was incubated at 37°C. For each analysis point, serum proteins were precipitated by adding 30 µL acetonitrile to 10 µL serum medium. The supernatant was separated by centrifugation at 4000 rpm, and then analyzed by radioHPLC or radioTLC. The supernatant contains over 95% of the activity of the initial aliquot.

7a. Stability of ^{125}I@BU 3 in HS

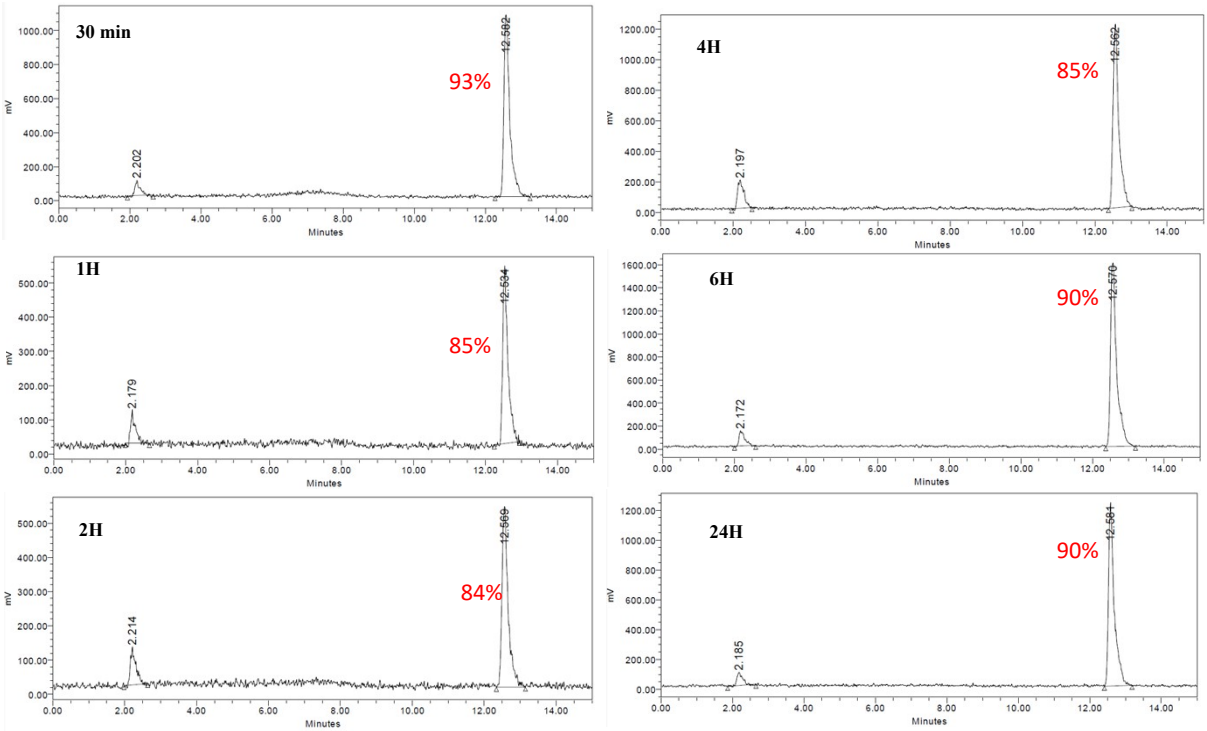

Figure S13: radioHPLC analysis of ^{125}I@**BU 3** in human serum at 37°C in fonction of the time

7b. Stability of ^{211}At@BU 4 in HS

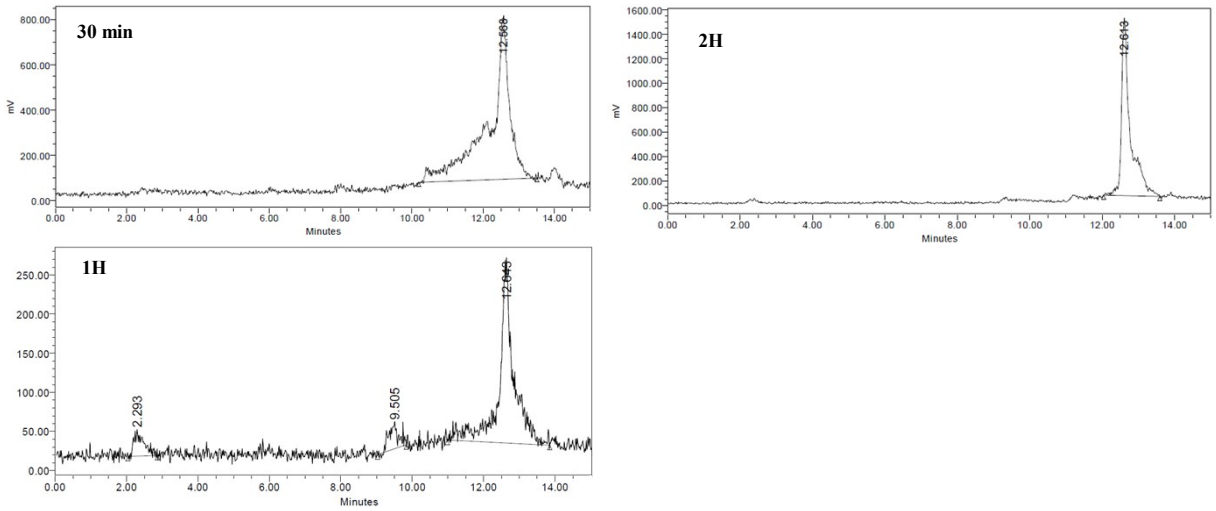

Figure S14a: radioHPLC analysis of ^{211}At@**BU 4** in human serum at 37°C after 30 min, 2h, 3h.

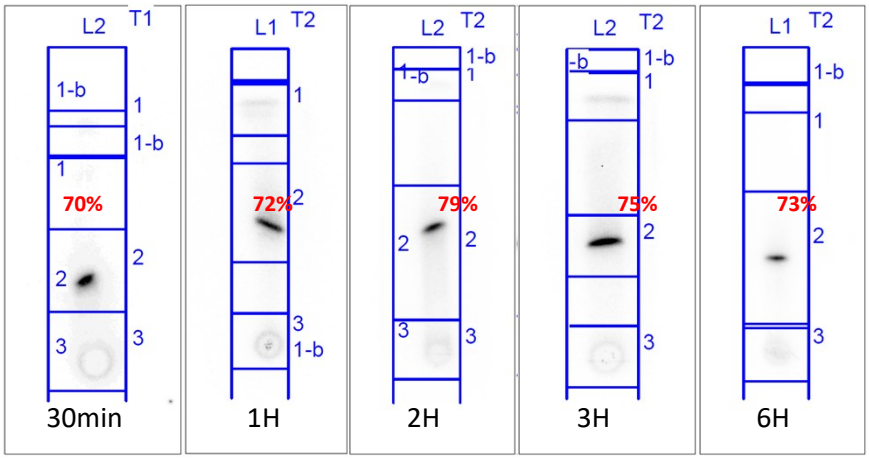

Figure S14b : radioTLC analysis of ^{211}At@BU 4 in human serum at 37°C after 30 min, 1h, 2h, 3h to 6 hours (elution with CH_2Cl_2/MeOH : 9/1).

8. Computational methods

8a. Geometry optimization

The geometry optimization of various anions binding with bambusuril were performed with the r^{2}SCAN-3c [4] composite density functional theory (DFT) method using the ORCA 5.0.4 program. [5] The approach combines the r^{2}SCAN meta-generalized-gradient approximation with triple-ζ Gaussian basis set and the semi-classical D4 and gCP correction potentials for London-dispersion and basis set superposition error.

8b. Energy Decomposition Analysis (EDA)

Analysis of the anion-bambusuril interaction has been performed combining a fragment approach to the molecular structure of the complex with the decomposition of the total bonding energy into separate components familiar to chemists:

$$\Delta E_{int.} = \Delta E_{elst} + \Delta E_{Pauli} + \Delta E_{oi}$$

The interaction energy $\Delta E_{int.}$ between two fragments A and B in a molecular system A-B is mainly partitioned in three terms, namely, (1) the quasiclassical electrostatic interaction ΔE_{elst} between the fragments, (2) the repulsive exchange (Pauli) interaction ΔE_{Pauli} between electrons of the two fragments having the same spin, and (3) the orbital (covalent) interaction ΔE_{oi}, which comes from the orbital relaxation and the orbital mixing between the fragments.[6] The orbital interaction accounts for charge transfer and polarization.

All computations were performed using ADF 2024.1[7] with DFT/revDOD-PBE-D4 [8], incorporating relativistic corrections via the ZORA approximation. TZ2P all-electron basis sets were employed at the ORCA-optimized geometries. This EDA framework also facilitates the calculation of the dispersion term, as well as short-range and long-range correlation effects included in the MP2 term. For the EDA, the selected fragments were the anion and the bambusuril cage.

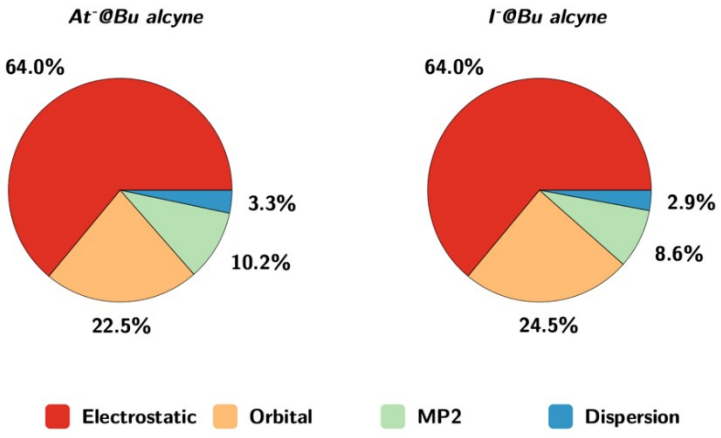

Figure S15: Percentages of the total stabilizing interaction energy (energy decomposition analysis).

8c. Decomposing anion-bambusuril cage interaction as atom and atomic pair contributions

Calculations were performed at the optimized geometry using the ORCA software, employing the ωB97M-V functional [9], a SARC basis set [10-11] and a ZORA Hamiltonian. All results were analyzed with Multiwfn (development version 3.8) software [12] using the Independent Gradient Model (IGM) based on Hirshfeld partitioning.

a) I^- @**BU 3** b) At^-@**BU 4**

Figure S16: The isosurface map visualizes the interaction regions between I^- and At^- anions with hydrogen atoms. The molecular structure is color-coded according to the contribution of various atoms to the interfragment interaction, using a Blue-Green-Red color scale. Atoms appearing more red indicate a greater involvement in the anion-bambusuril cage interaction, highlighting regions of stronger interaction.

8d. Cavity

The cavity size of bambusuril was determined using the MoloVol software[13] based on the ORCA-optimized geometry.

Full cavity **Central cavity**

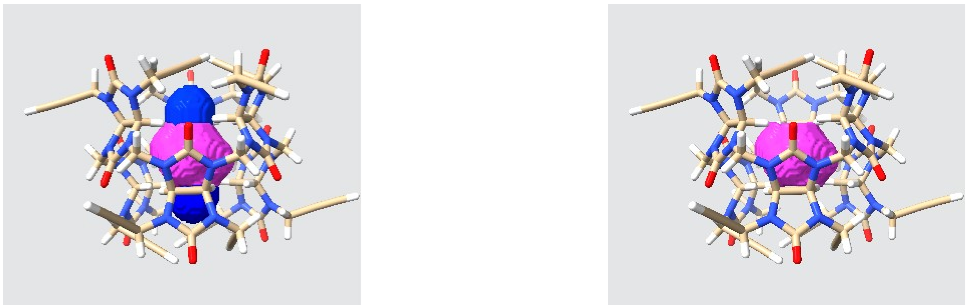

Figure S17 : Propargyl$_{12}$BU[6] cavity **BU 1** shape visualized with CHIMERA.[14]

Note: in our 2018 study [2] we measured the total cavity size. In this work, we specifically analyze the central cavity volume, as MoloVol provides a more accurate estimation of the cation's cavity volume.

Quantum chemical calculations were also employed to determine the volume of the central bambusuril cavity, both for the empty cage and with the anions encapsulated (See Figure 5 and the Supporting Information for further details).

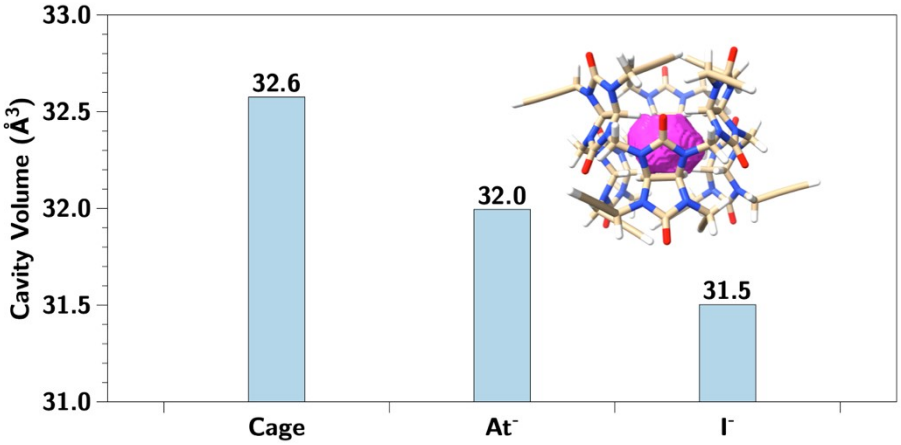

Figure S18 : Volumes of the central BU cavity **BU 1**

The volume of the central cavity in the empty BU's cage **BU 1** was determined to be 32.6 Å. In the presence of astatine and iodide anions, the cavity volume decreased to 32.0 Å and 31.5 Å, respectively. The smaller cavity size observed with iodide compared to astatine suggests a stronger interaction between the iodide anion and the cage, consistent with the interaction energy analysis.

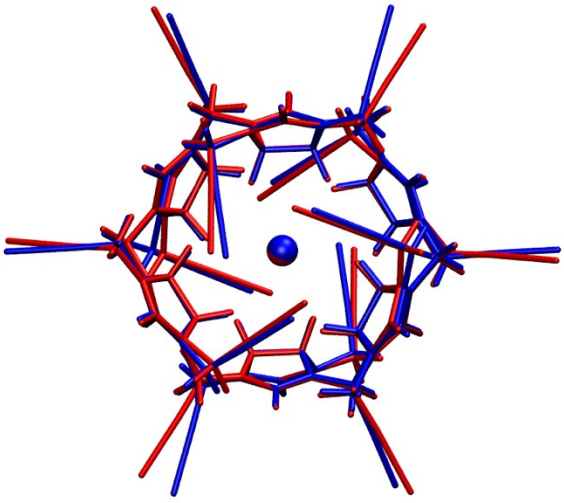

Figure S19 : Calculated structures (red color) vs. the experimentally reported crystal structure (blue color, Ref. 18) for the iodide compound.

9. Bibliography

[1] M. Lafosse, E. Cartier, K. Solmont, J. Rivollier, D. Azazna, P., Thuéry, Y. Boulard, A. Gontier, J.-B. Charbonnier, B. Kuhnast, M.-P. Heck, M.-P. *Org. Lett*., **2020**, *22*, 3099-3103.

[2] D. Azazna, M. Lafosse, J. Rivollier, J., Wang, I. Ben Cheikh, M. Meyer, P. Thuéry, J.-P. Dognon, G. Huber, M.-P. Heck, M.-P. *Chem. Eur. J.* **2018,** 24, 10793-10801.

[3] P. Thordarson *Chem. Soc. Rev.* **2011**, *40*, 1305-1323.

[4] S. Grimme, A. Hansen, S. Ehlert, J.-M. Mewes, *J. Chem. Phys.,* 2021, **154**, 064103.

[5] F. Neese, *WIREs Comput. Mol. Sci.,* 2022, **12**, e1606.

[6] F. M. Bickelhaupt, E. J. Baerends, *In: Rev. Comput. Chem., K.B. Lipkowitz and D.B. Boyd, Eds., Wiley, New York*, 2000, **15**, 1-86.

[7] ADF 2024.1, SCM, Theoretical Chemistry, Vrije Universiteit, Amsterdam, The Netherlands, http://www.scm.com

[8] G. Santra, N. Sylvetsky, J. M. L. Martin, *J. Phys. Chem. A,* 2019, **123**, 5129–5143.

[9] N. Mardirossian, M. Head-Gordon, *J. Chem. Phys.*, 2016, **144**, 214110.

[10] J. D. Rolfes, F. Neese, D. A. Pantazis, *J. Comput. Chem.*, 2020, **41**,1842-1849.

[11] D. A. Pantazis, F. Neese, *Theor. Chem. Acc.*, 2012, **131**, 1292.

[12] T. Lu, *J. Chem. Phys.*, 2024, **161**, 082503.

[13] J. B. Maglic, R. Lavendomme, *J. Appl. Cryst.*, 2019, **55**, 1033-1044.

[14] E. F. Pettersen, T. D. Goddard, C. C. Huang, G. S. Couch, D. M. Greenblatt, E. C. Meng, T. E. Ferrin, *J. Comput. Chem. 2004*, **25**, 1605-1612.

[15] S. Lindegren, *Cancer Biother Radiopharm*., 2020, **35**, 425–436.